

Article

Mechanism of Direct C-H Arylation of Pyridine via a Transient Activator Strategy: A Combined Computational and Experimental Study

Feiyun Jia, Changzhen Yin, Yang Zeng, Rui Sun, Yi-Cen Ge, Dingguo Xu, Ruixiang Li, Hua Chen, Chunchun Zhang, and Haiyan Fu

J. Org. Chem., **Just Accepted Manuscript** • Publication Date (Web): 24 Jul 2018

Downloaded from <http://pubs.acs.org> on July 24, 2018

Just Accepted

"Just Accepted" manuscripts have been peer-reviewed and accepted for publication. They are posted online prior to technical editing, formatting for publication and author proofing. The American Chemical Society provides "Just Accepted" as a service to the research community to expedite the dissemination of scientific material as soon as possible after acceptance. "Just Accepted" manuscripts appear in full in PDF format accompanied by an HTML abstract. "Just Accepted" manuscripts have been fully peer reviewed, but should not be considered the official version of record. They are citable by the Digital Object Identifier (DOI®). "Just Accepted" is an optional service offered to authors. Therefore, the "Just Accepted" Web site may not include all articles that will be published in the journal. After a manuscript is technically edited and formatted, it will be removed from the "Just Accepted" Web site and published as an ASAP article. Note that technical editing may introduce minor changes to the manuscript text and/or graphics which could affect content, and all legal disclaimers and ethical guidelines that apply to the journal pertain. ACS cannot be held responsible for errors or consequences arising from the use of information contained in these "Just Accepted" manuscripts.



ACS Publications

is published by the American Chemical Society, 1155 Sixteenth Street N.W., Washington, DC 20036

Published by American Chemical Society. Copyright © American Chemical Society. However, no copyright claim is made to original U.S. Government works, or works produced by employees of any Commonwealth realm Crown government in the course of their duties.

Mechanism of Direct C–H Arylation of Pyridine via a Transient Activator Strategy: A Combined Computational and Experimental Study

Feiyun Jia,^{†,‡} Changzhen Yin,[†] Yang Zeng,[†] Rui Sun,[†] Yi-Cen Ge,[§] Dingguo Xu,

Ruixiang Li,[†] Hua Chen,[†] Chunchun Zhang,^{*,||} and Haiyan Fu^{*†}

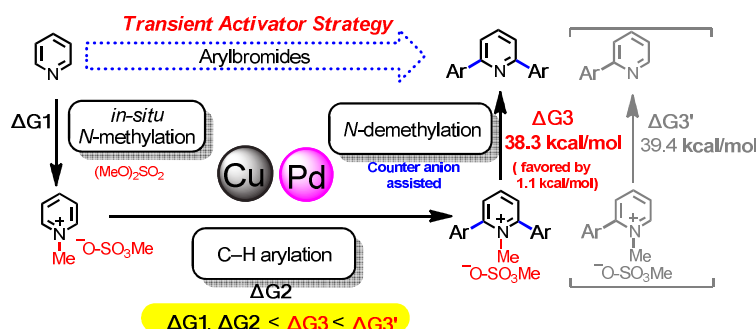
[†] Key Laboratory of Green Chemistry & Technology, Ministry of Education College of Chemistry, Sichuan University, Chengdu 610064, P. R. China.

[‡] School of Basic Medical Sciences, North Sichuan Medical College, Nanchong, Sichuan 637007, P. R. China.

[§] Division of Chemistry and Biological Chemistry, Nanyang Technological University, 21 Nanyang Link, Singapore 637371

^{||} Analytical & Testing Center, Sichuan University, Chengdu, Sichuan 610064, P. R. China.

* To whom corresponding author should be addressed: scufhy@scu.edu.cn (FX) and cczh@scu.edu.cn (CZ)



ABSTRACT: Recently, we realized the highly selective one-pot synthesis of 2, 6-diarylpiperidines by using a Pd-catalyzed direct C–H arylation approach via a transient

activator strategy. Although methylation reagent as a transient activator and Cu(I) salt or oxide were found prerequisite, details regarding the mechanism remained unclear. In this article, DFT calculations combined with experimental investigations were carried out to elucidate the principle features of this transformation. The results reveal: (1) the origin of the exquisite di-arylation selectivity of the pyridine under the transient strategy; (2) the possible demethylating reagent to be the counter anion of the pyridinium salt; (3) the reason why Cu₂O is a better Cu(I) resource than others.

KEYWORDS: DFT study, C–H functionalization, N-methylation, transmetalation, copper.

■ INTRODUCTION

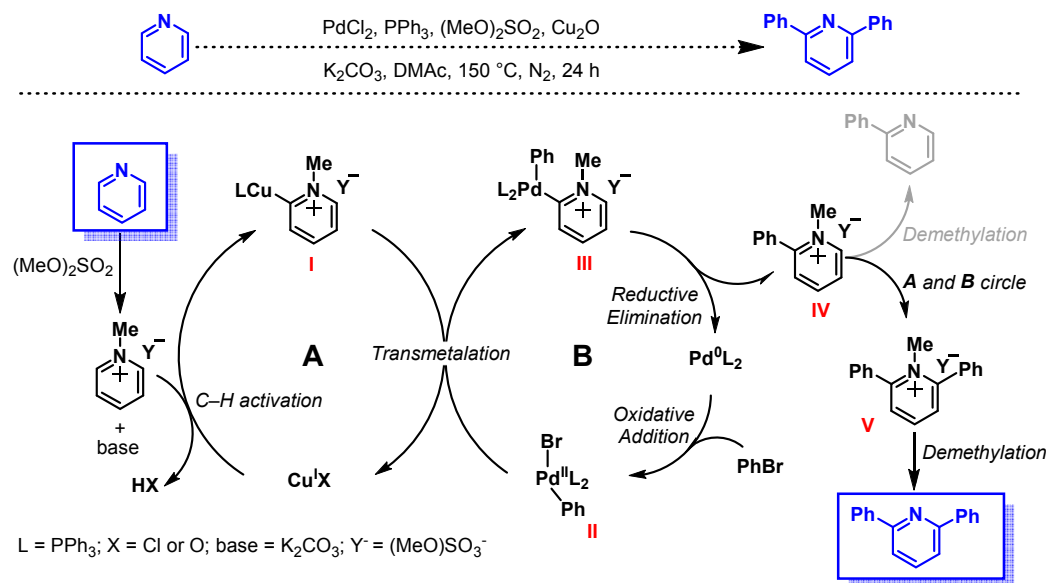
Arylpyridines are important synthetic motifs which are widely employed in a variety of bioactive natural products and pharmaceutical synthesis, as well as material sciences.¹⁻⁶ As the synthesis of arylpyridines remains a compelling goal in modern chemical research,⁷⁻⁹ transition-metal-catalyzed direct C–H arylation, enabling one-step functionalization of pyridines, has become the most attractive method. However, this straight-forward transformation often suffers from low reactivity and poor selectivity, due to the electron deficiency and strong Lewis basicity of pyridines. In such situation, the transition-metal-catalyzed direct C–H arylation remains rather challenging and still necessary to be further explored.¹⁰⁻¹³

In order to improve the reactivity and selectivity, pre-activation strategy has been widely applied in pyridine arylation reactions.¹⁴⁻¹⁷ Although significant progress has been achieved by Fagnou, Hartwig, Charrette, Berman and other groups,¹⁸⁻²² the

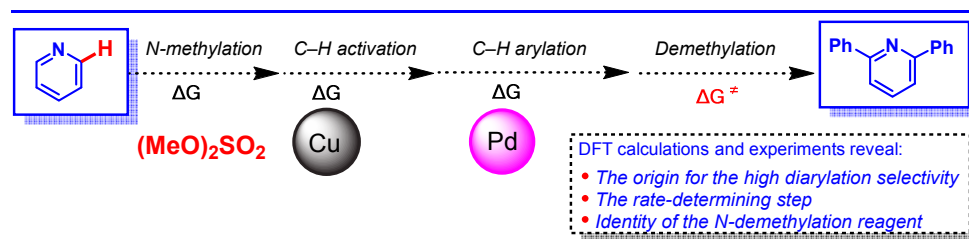
problem arises as removing the pre-installed activating groups is required to afford the target products.²³ In recent years, traceless or transient directing group strategies have been discovered and applied extensively in organic synthesis.²⁴⁻³⁰ Inspired by these precedent discoveries, we successfully developed a transient activator strategy to realize the highly selective Pd-catalyzed C–H 2,6-diarylation of pyridines.³¹ Methylating reagent as the transient activator was found to define the success of the reaction, while Cu(I) source as the additive was also important. Generally, it is believed that *N*-methylation, C–H arylation and *N*-demethylation occur sequentially in a one-pot manner during the process.

Scheme 1. Direct C–H Arylation of Pyridine via a Transient Activator Strategy

*The Proposed Mechanism Based on Experimental Results in Previous Work*³¹



Understanding of the Mechanism by DFT Calculations and Experiments in This Work



A putative mechanism is proposed in Scheme 1. The pyridinium salt derived from *in situ* N-methylation reacts with LCuCl ($\text{L}=\text{PPh}_3$) in the presence of base to afford the pyridinium-Cu(I) complex **I**. Meanwhile, palladium complex **II** is generated via oxidative addition of Pd(0)L_2 with PhBr . After transmetalation between **I** and **II**, the palladium intermediate **III** is furnished, which further gives rise to the monoarylation product **IV** by the subsequential reductive elimination. The N-methylpyridinium salt **IV** either undergoes demethylation to afford the monoarylated pyridine, or re-enters the catalytic cycle to give diarylated pyridinium salt **V** which eventually furnishes the major product 2, 6-diarylpiperidine after demethylation. Interestingly, our reaction requires an elevated temperature of 150 °C, much higher than the usual C–H functionalization reactions.^{32–35} Although experimental efforts have been made to understand the mechanistic details, some key issues are still not fully addressed, such as rate-limiting step, temperature dependence and ways to improve the yield of the reaction.

Theoretical methods represent alternative ways to tackle mechanistic problems in chemical reactions.³⁶ Recently, great progress has been made via theoretical calculation on the mechanistic investigations of C–H bond functionalization by Houk, Wu, Lin and other groups.^{37–41} In this work, intensive density functional theory

(DFT) calculations are employed in combination with experimental characterizations. We aim to find the plausible answers to some mechanistic issues of the transient activator strategy for Pd-catalyzed C–H arylation of pyridine: (1) the origin for the high diarylation selectivity; (2) the rate-determining step of the reaction; (3) the identity of *N*-demethylation reagent in the final step, which could be solvent (DMAc: *N,N*-dimethylacetamide), ligand (PPh₃) or counterion (MeOSO₃[−]); (4) the requirement of the high reaction temperature of 150 °C. Herein, we detail the results of performed investigations on the above questions to acquire a better understanding of the inner workings relating to this direct arylation reaction. We hope that our explorations will provide an opportunity to improve the efficiency of arylpyridine synthesis and extend the current system to other *N*-heterocyclic compounds.

■ COMPUTATIONAL DETAILS

Full geometry optimizations were carried out using B3LYP⁴²⁻⁴³ exchange correlation functional in gas phase with mixed basis sets. In particular, the effective core potentials (ECPs)⁴⁴ of Hay and Wadt with double- ζ valence basis sets (LanL2DZ) was applied for atoms of palladium, copper, bromine, and potassium, while the double- ζ split-valence 6-31G(d) basis set for the rest of atoms. Vibrational frequencies were calculated to confirm minima with all positive frequencies and transition states with only one imaginary frequency. Meanwhile, thermodynamic quantities like thermal corrections to enthalpy and Gibbs free energy were performed as the same level of theory. Intrinsic reaction coordinates (IRC)⁴⁵⁻⁴⁶ were applied to connect all stationary states. In order to obtain the reactive energetic profiles, single-point

calculations were carried out using M06⁴⁷⁻⁴⁸ functional based on the B3LYP optimized geometries. The M06 functional has been demonstrated to be particularly suitable for describing copper containing systems.⁴⁹⁻⁵² In such calculations, mixed basis sets consisting of SDD for palladium, copper, bromine and potassium and 6-311+G (d, p) basis set for other atoms were applied. The solvation model density (SMD)⁵³ continuum method was used to account for the solvent effects in all single-point energy calculations. Consistent with the experimental conditions, *N*, *N*-Dimethylacetamide was selected as the solvent in our computation.

Natural Population Analysis (NPA) charge calculations for some selected species were employed at the M06//B3LYP single point level of theory within the SMD solvation model. The temperature-dependent enthalpy corrections and the entropy effects were computed at 298K and 1 atmosphere of pressure. All calculations were performed using Gaussian 09 suite of program.⁵⁴

■ RESULTS AND DISCUSSION

***N*-Methylation.** On the basis of the catalytic mechanism proposed in Scheme 1, we first investigated the *N*-methylation of pyridine with (MeO)₂SO₂ to form the intermediate **2**. This is a typical S_N2 reaction, in which the free-energy barrier to complete the *N*-methylation via transition state **TS1** was calculated to be 16.9 kcal/mol according to Figure 1. The methyl group migrates from (MeO)₂SO₂ to pyridine by Walden inversion. **TS1** features a nearly planar methyl group at the middle of pyridine and –OSO₂OMe group from Figure 1. Once the bond between pyridine N atom and the methyl group is formed, the dissociation of this methyl group

from sulfate is accelerated. In fact, a relatively large exothermicity of 23.3 kcal/mol for the *N*-methylation reaction was found, which indicated that the reaction is thermodynamically favorable.

Charge development for some key atoms deserves further discussion. Charges of pyridine and *N*-methylpyridine were investigated using Natural Population Analysis (NPA) approach. As shown in Scheme 2, along with methylation at the nitrogen atom of pyridine, hydrogen atoms on the pyridine ring become more acidic, *esp.* the 2, 6-positions. The NPA charge of the hydrogen atoms increases from 0.198 to 0.250 upon the formation of pyridinium salt. It is consistent with the experimental finding that the reactivity of pyridine is significantly enhanced after being methylated, especially at the *ortho*-positions.³¹

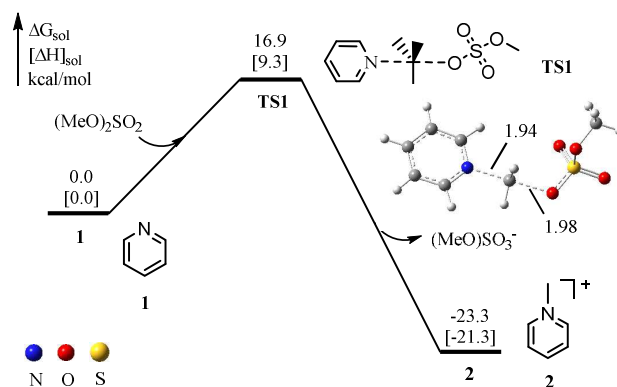
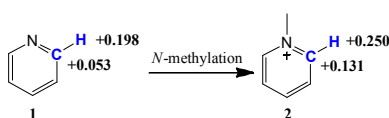


Figure 1. Reaction energy profile of *N*-methylation of pyridine with $(\text{MeO})_2\text{SO}_2$.

Scheme 2. NPA charge analysis to rationalize the H atomic acidity change at the 2-position of pyridine before and after *N*-methylation.



C–H Arylation. The following step is the C–H arylation of the corresponding *N*-methylpyridinium salt. In comparison to pyridine, the pyridinium salt has increased proton acidity of C–H bond,³¹ and therefore increased C–H arylation reactivity. It is proposed that this process consists of copper-induced activation of C–H bond and palladium catalyzed arylation. With regard to the C–H activation step, two possible pathways need to be systematically evaluated, which mainly differ in the role of base according to precedent studies on base-assisted C–H activation reactions.⁵⁵⁻⁵⁶ In consistency with our arylation selectivity, we only investigated the activation of C₂–H in this section.

In pathway **I** (Figure 2, the black line), a double salt KCl·LCuCO₃K **4** with the structure shown in Figure 2, is generated first via ligand exchange of chloride with carbonate (K₂CO₃). The reaction is thermodynamically favored due to the large exothermicity (–10.9 kcal/mol) and the absence of energy barrier height. The leaving of KCl from the double salt gives LCuCO₃K **5**, with which a concerted metalation-deprotonation (CMD)⁵⁷ process of **2** occurs subsequently. It is indicated that the proton transfers from the C2-position of pyridinium salt to the carbonate via a distorted six-membered ring transition state **TS2** which produces the copper(I) *N*-methylpyridinium intermediate **6**. The overall free-energy barrier for this base-assisted pathway **I** is calculated to be 17.4 kcal/mol.

On the contrary, another C–H activation pathway **II** (Figure 2, the blue line) does not need to generate the double salt **4**. Instead, K₂CO₃ as base directly participates the C–H activation without the assist of CuCl. Basically, pathway **II** is believed involving

two processes: (a) proton abstraction from pyridinium salt with potassium carbonate, (b) transmetalation to give the copper(I)-pyridinium complex. First, via a six-membered ring transition state **TS3**, proton transfer occurs at the C2-position of the pyridinium ring with the oxygen atom of carbonate, which affords the potassium *N*-methylpyridinium intermediate **7**. Calculations demonstrate that the free-energy barrier of this step is 14.4 kcal/mol. After that, intermediate **7** undergoes transmetalation with copper (I) salt to form **6** via the transition state **TS4**, with a relatively low free-energy barrier of 1.5 kcal/mol. As shown in Figure 2, the overall free-energy barrier for the pathway **II** is calculated to be 14.5 kcal/mol, which is much lower than pathway **I**. Thus, the kinetically favored pathway **II** is more likely responsible for C–H activation process, whereas K₂CO₃ acts as a base at the very first beginning.

Meanwhile, we have also examined the direct C–H activation between LCuCl and *N*-methylpyridinium salt in the absence of any additional bases. The corresponding energy barrier is found to be 45.4 kcal/mol (see SI, Figure S1). It is much higher than the base-assisted pathway **II**, which is rationalized as the carbonate is a stronger base than chloride. In such situation, our computation clearly demonstrates the importance of K₂CO₃ as the base in the C–H activation step with the current system.

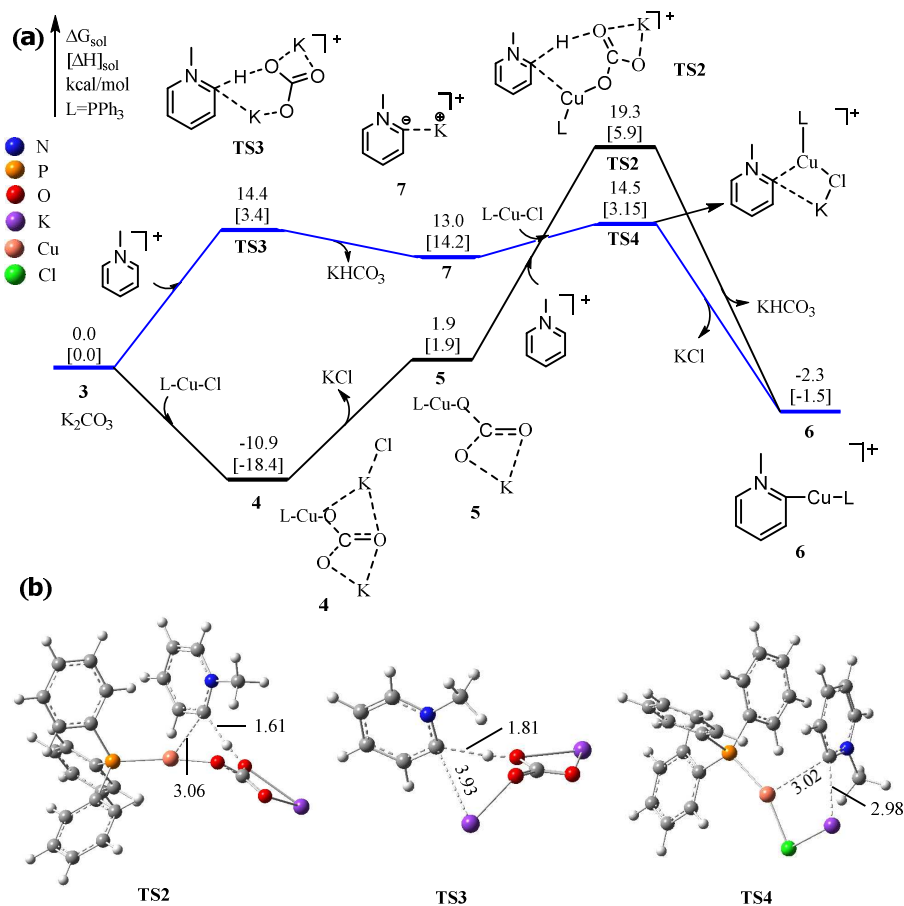


Figure 2. (a) Energy profile for the C–H activation of *N*-methylpyridine, involving two base-assisted pathways. (b) Computed structures of transition states with select bond distances shown in Å.

In the above calculations, CuCl is chosen as the additive. In our previous work, we found that Cu₂O exhibited similar efficiency to afford arylation products but with superior diarylation selectivity comparing to CuCl.³¹ Herein, the C–H activation reaction involving Cu₂O is further discussed, while the role of PPh₃ is also investigated. As summarized in Figure 3, two putative C–H activation pathways were computed, with and without PPh₃, respectively. K₂CO₃ is not included in the present simulation. Similar to the previous base-assisted C–H activation, the current step also

features a CMD mechanism. In the first pathway **III** (Figure 3, the black line), the oxygen atom of Cu₂O directly abstracts the most acidic proton of pyridinium to form the intermediate **8** via the transition state **TS6** with a 12.2 kcal/mol barrier. In the second pathway **IV** (Figure 3, the blue line), the deprotonation occurs in the presence of LCu₂O to give the intermediate **6** via the transition state **TS5**. In the presence of ligand PPh₃, the free-energy barrier is further reduced to 10.7 kcal/mol, revealing the necessity of PPh₃ to enhance the reactivity. The advantage in kinetics by 3.8 kcal/mol implies the superiority of basic Cu₂O in the presence of PPh₃ for C–H activation compared to CuCl in pathway **II**. These computational results revealed the Cu₂O is an additive superior to CuCl. In addition, a series of deuterium incorporation experimental results for pyridinium salt **i** as demonstrated in Table 1 further supported above conclusion: Nearly no deuterium incorporation was observed when the pyridinium salt **i** was treated with CuCl alone in D₂O (Table 1, entry 1), while 44% deuterium incorporation product (**ia** and **iaa**) could be achieved with the assistance of K₂CO₃ (Table 1, entry 2), moreover, the percentage was significantly increased to 92% when replacing CuCl with Cu₂O (Table 1, entry 3).

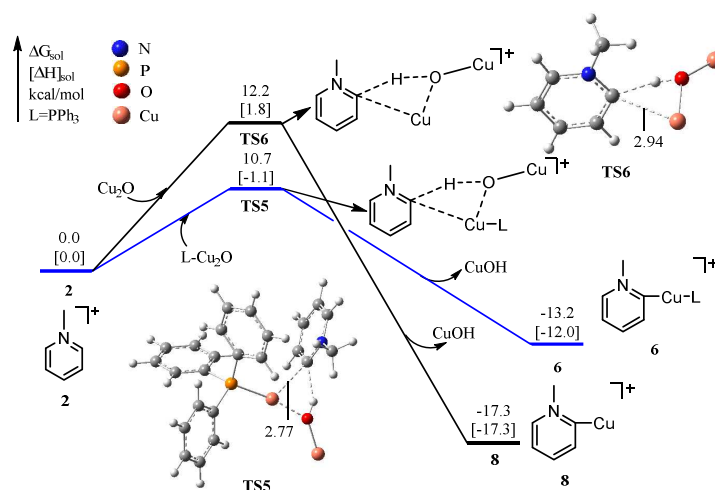


Figure 3. Reaction energy profiles of the C–H activation of *N*-methylpyridium with Cu₂O and

LCu₂O.

Table 1. Deuterium Incorporation Study ^a

entry	additive	base	D incorporation (%)
1 ^b	CuCl	-	N.D.
2 ^b	CuCl	K ₂ CO ₃	44
3	Cu ₂ O	K ₂ CO ₃	92

^a Reaction condition: **i** (0.25 mmol, 1.0 equiv.), additive (0.125 mmol, 0.5 equiv.), base (0.25 mmol, 1 equiv.), D₂O (0.3 mL), 100 °C for 1 h under N₂. Yields were determined by ¹H NMR analysis of a crude product with CH₂Br₂ as internal standard. ^b 0.25 mmol additive was used.

The next step after C–H activation is the palladium catalyzed arylation which includes oxidative addition, transmetalation and reductive elimination. Figure 4(a) shows the energy profile for the complete catalytic cycle. The oxidative addition of PhBr to L₂Pd(0) is a concerted process via a three-membered ring transition state **TS7**,

which requires 17.9 kcal/mol to generate the Pd(II) intermediate **10**. Subsequently, the complex **10** releases one ligand (PPh₃) and interacts with complex **6** to form the metastable adduct **11**. With a low energy barrier of 1.5 kcal/mol, the transmetalation then occurs easily via a four-membered ring transition state **TS8**, which finally gives the intermediate **12**. Interestingly, our calculation results suggest that in **TS8** $d_{\text{Pd-Br}}$ is elongated to 2.78 Å and $d_{\text{Cu-C}}$ changes to 2.71 Å, from 2.65 Å and 1.96 Å in the intermediate **10** and intermediate **6**, respectively. Thus, the ligand transfer of *N*-methylpyridinium from Cu to Pd is facilitated. From **12**, reductive elimination takes place via a three-membered ring transition state **TS9** with the free-energy barrier of 6.7 kcal/mol, leading to 2-phenyl-*N*-methylpyridinium salt and recovering the catalyst **9** (L₂Pd). The palladium catalytic cycle is exergonic by 39.5 kcal/mol, which indicates the whole process is thermodynamically favorable. All structures of transition states involved in the palladium catalytic cycle are illuminated in Figure 4(b).

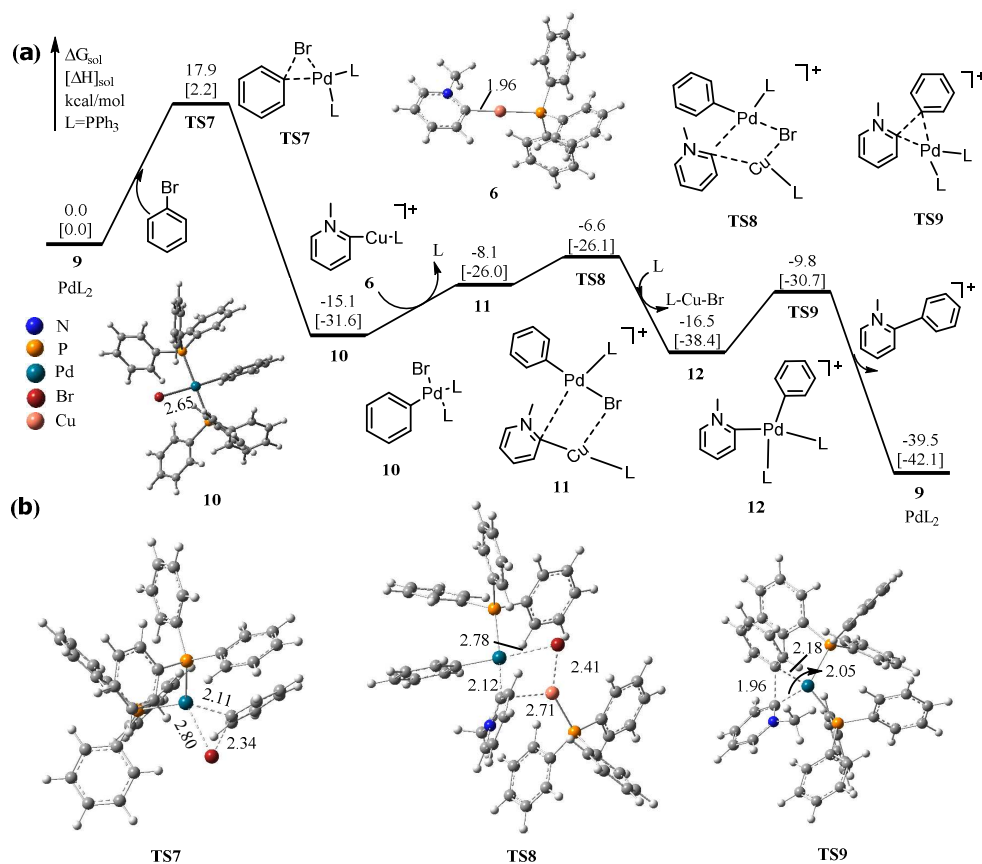
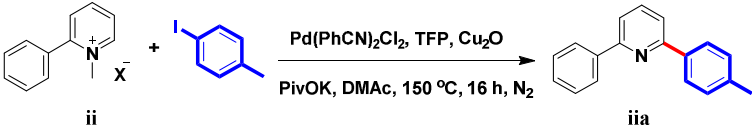


Figure 4. (a) Energy profile calculated for the Palladium catalytic cycle. (b) Computed structures of transition states with selected bond distances shown in Å.

***N*-Demethylation.** Once the 2-aryl-*N*-methylpyridinium salt is formed, two possible processes might further take place with our system. One features a direct demethylation reaction to generate the monoarylated pyridine, while the other is assumed to re-enter the catalytic cycle of diarylation. Generally, many methods have been reported to demethylate the *N*-methylpyridinium salts.⁵⁸⁻⁵⁹ Among them, the most common way is the $\text{S}_{\text{N}}2$ -type nucleophilic attack on pyridinium salts with elevated reaction temperature.⁶⁰ In our system, there are multiple potential nucleophiles, such as the ligand PPh_3 , the solvent DMAc and the counterion of the pyridinium salts (MeOSO_3^-). Moreover, a higher temperature of 150 °C is required in

the demethylation step with our system. In order for a better understanding of the detailed mechanism, a careful exploration of the demethylation step is highly desired. Thus, the demethylation processes were then simulated based on density functional theory, with the corresponding energetic profiles plotted in Figure 5. Clearly, the lowest energy barrier ($\Delta G = 33.5$ kcal/mol) is observed in the case of PPh_3 , which has been reported as an efficient demethylating reagent.⁵⁸ In the current system, however, PPh_3 is unlikely the main demethylation reagent because only 0.2 equivalents (based on the pyridine) was employed and hence seriously inadequate. On the other hand, DMAc is also less likely due to the high energy barrier (40.6 kcal/mol). Therefore, we believe that the counter anion $(\text{MeO})\text{SO}_3^-$ actually acts as the demethylating reagent. Indeed, our calculation shows that the activation energy is 2.3 kcal/mol lower than the case of DMAc. To further support our hypothesis, we designed a series of coupling reaction between 4-tolyl iodide and *N*-methyl-2-phenylpyridinium salts **ii** bearing different counter anions. Impressively, different yields of arylation products were observed, which have good correlations with free-energy barriers of the *N*-demethylation of the corresponding diaryl pyridinium salts: the lower energy barrier led to higher yield (as shown in Table 2).

Table 2. The Effect of Counter Anions of the Pyridinium **ii** on Yield ^a



entry	Y ⁻	yield (%) ^b	$\Delta G^{\text{cal}} [\Delta H^{\text{cal}}]$ (kcal/mol) ^c
1	I ⁻	83	27.7 [20.7]
2	NO ₃ ⁻	67	33.4 [22.7]

3	CF_3COO^-	61	34.7 [22.4]
4	TsO^-	47	37.0 [25.8]
5	$\text{CH}_3\text{OSO}_3^-$	41	39.1 [27.9]

^a Reaction conditions: **ii** (0.5 mmol, 1 equiv.), 4-tolyl iodide (1.0 mmol, 2 equiv.), $\text{Pd}(\text{PhCN})_2\text{Cl}_2$ (5 mol%), TFP (10 mol%), Cu_2O (0.25 mmol, 0.5 equiv.), PivOK (1.0 mmol, 2 equiv.), 150 °C, 16 h, under N_2 ; TFP = tri-2-furylphosphine; ^b Isolated yields; ^c The calculated free-energy barriers for *N*-demethylation of the diaryl pyridinium salts. See the SI, figure S2.

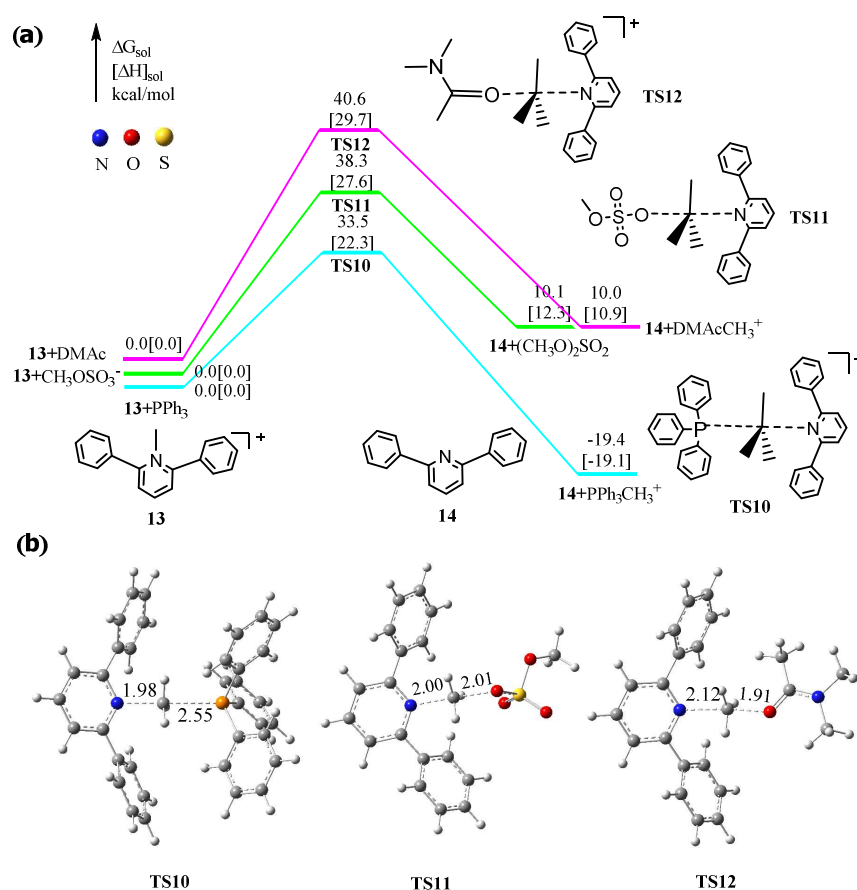


Figure 5. (a) Energy profiles calculated for the demethylation reactions with different demethylating reagents. (b) The computed structures of transition states with selected bond distances shown in Å.

Rate-determining Step and Site-selectivity. The overall free-energy profile of the

reaction is shown in Figure 6. For clarification, all energy barrier heights are scaled in accord with the reactant **1** and (MeO)₂SO₂. As demonstrated in Figure 6, the barrier of the demethylation step is much higher than the others. Thus, the calculation result well explains why our system requires such a high reaction temperature which differs from the previous reports, and *N*-demethylation is proposed to be the rate-determining step.^{32–35} Since it has been reported that the electron-donating group on the pyridinium ring would greatly slow down the *N*-demethylation process,⁵⁸ 4-dimethylaminopyridine (DMAP) was further tested as the substrate with our system (Table 3). As expected, DMAP exhibited a relatively low reactivity, with only 36% yield of diarylated product obtained after 24 h. If the reaction time was prolonged to three days, the yield was successfully increased to a moderate level of 65%. The free-energy barrier for demethylation of the corresponding *N*-methyl diarylated pyridinium salt is calculated as high as 43.4 kcal/mol (see SI, Figure S3), which possibly accounts for the requirement of a longer reaction time. In a word, the experimental results help to support *N*-demethylation as the rate-determining step.

In order to gain insights into the origin of high diarylation selectivity, we further carried out more computational investigations on the related steps. After the first reaction cycle, the monoarylated *N*-methylpyridinium salt is supposed to either undergo the demethylation to afford the monoarylated pyridine or re-enter the second catalytic arylation cycle to produce 2, 6-diaryl-*N*-methylpyridinium salt. According to Figure 6, the barrier height for demethylation of the monoarylated pyridinium salt is much higher than the other steps. Therefore, re-entering the catalytic cycle is more

1
2
3
4 favored. Furthermore, the barrier of demethylation process for diarylation product is
5
6 found slightly lower than that for the monoarylated counterparts (38.3 vs. 39.4
7
8 kcal/mol), possibly due to the releasing of more strain in the former case.⁵⁸ Hence, we
9
10 can conclude that the demethylation process prefers to occur after the diarylation,
11
12 rather than the monoarylation, which deciphers the observed di-/mono-arylation
13
14 selectivity with this transient activator strategy.
15
16

17
18 **Table 3.** The Effect of Reaction Time on Yield ^a

19
20
21
22
23
24
25

26
27

entry	reaction time (h)	yield (%) ^b
1	24	36
2	48	59
3	72	65

28
29
30
31
32
33

34 ^a **iii** (0.5 mmol), 4-tolyl iodide (1.5 mmol), PdCl₂ (5 mol %), PPh₃ (10 mol %), K₂CO₃ (4.0 equiv),
35
36 (MeO)₂SO₂ (0.8 equiv), Cu₂O (0.5 equiv), DMAc (2.5 mL), 150 °C, 4 Å MS (100 mg), 150°C,
37
38 under N₂; ^b Isolated yields.
39
40
41

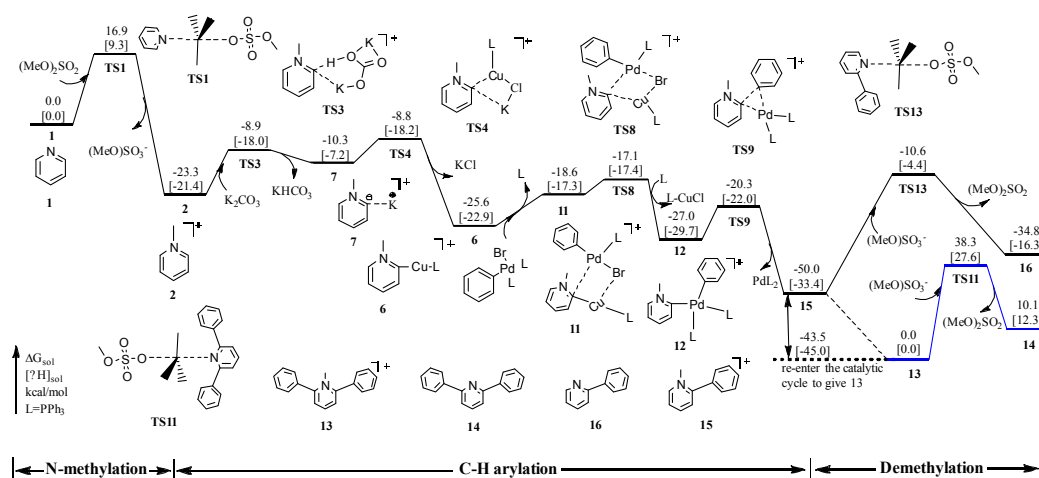


Figure 6. The overall energy profile calculated for the direct C–H arylation of pyridine.

■ CONCLUSIONS

In this work, by using DFT calculations combined with experimental investigations, we disclose the detail mechanism of Pd-catalyzed C–H arylation of pyridine via the transient activator strategy. The whole process comprises three key steps, including *N*-methylation, C–H arylation, and *N*-demethylation. The *N*-methylation enhances the acidity of protons on pyridine significantly, thereby improving the arylation reactivity. The resulting pyridinium salt reacts with LCuCl in the presence of the base (K_2CO_3) to give copper(I) pyridinium intermediate. Herein, two possible pathways for C–H activation step were calculated. The concerted metalation-deprotonation with K_2CO_3 followed by transmetalation with Cu(I) species, with a lower free-energy barrier of 14.5 kcal/mol, is therefore the more favorable pathway. From the resulting Cu(I) pyridinium species, the transmetalation with palladium and the subsequent reductive elimination occur to give the first monoarylation product. Between the following two competitive pathways, the calculation results suggest that monoarylation product undergoes the second arylation first rather than being directly demethylated. Selectively affording the diarylation product is more favored in the aspect of energetics, which is well consistent with our previous explorations. In addition, according to our calculations and experimental investigations, we believe that the counter anion Y^- ($MeOSO_3^-$) is more likely to be the demethylation reagent.

■ SUPPORTING INFORMATION

Supplementary experimental data.

Energy profile for the C-H activation of N-methylpyridine with CuCl (or CuCl-L) without base-assisted.

Energy profiles for the N-demethylation reactions of the three diaryl pyridinium salts.

Energy profiles of the rate-determining step of DMAP diarylation reaction.

Cartesian coordinates, computed total energies, enthalpy and Gibbs free energy of optimized structures.

■ ACKNOWLEDGEMENT

This work was funded by the National Natural Science Foundation of China (No. 21473117, No. 21572137) and the Key Program of Sichuan Science and Technology Project (No. 2018GZ0312). Some of the results described in this work were obtained with the help of the Supercomputing Center of Chinese Academy of Science.

■ REFERENCES

1. Desimoni, G.; Faita, G.; Quadrelli, P., Pyridine-2,6-bis(oxazolines), Helpful Ligands for Asymmetric Catalysts. *Chem. Rev.* **2003**, *103*, 3119–3154.
2. Henry, G. D., De novo synthesis of substituted pyridines. *Tetrahedron.* **2004**, *60*, 6043–6061.
3. Bull, J. A.; Mousseau, J. J.; Pelletier, G.; Charette, A. B., Synthesis of pyridine and dihydropyridine derivatives by regio- and stereoselective addition to N-activated pyridines. *Chem. Rev.* **2012**, *112*, 2642–2713.
4. Wang, Y.-F.; Chiba, S., Mn(III)-Mediated Reactions of Cyclopropanols with Vinyl

- Azides Synthesis of Pyridine and 2-Azabicyclo[3.3.1]non-2-en-1-ol Derivatives. *J. Am. Chem. Soc.* **2009**, *131*, 12570–12572.
5. Hagui, W.; Besbes, N.; Srasra, E.; Soulé, J.-F.; Doucet, H., Direct access to 2-(hetero)arylated pyridines from 6-substituted 2-bromopyridines via phosphine-free palladium-catalyzed C–H bond arylations: the importance of the C6 substituent. *RSC Adv.* **2016**, *6*, 17110–17117.
6. Isley, N. A.; Wang, Y.; Gallou, F.; Handa, S.; Aue, D. H.; Lipshutz, B. H., A Micellar Catalysis Strategy for Suzuki–Miyaura Cross-Couplings of 2-Pyridyl MIDA Boronates: No Copper, in Water, Very Mild Conditions. *ACS Catal.* **2017**, *7*, 8331–8337.
7. Carey, J. S.; Laffan, D.; Thomson, C.; Williams, M. T., Analysis of the reactions used for the preparation of drug candidate molecules. *Org. Biomol. Chem.* **2006**, *4*, 2337–2347.
8. Schlosser, M.; Mongin, F., Pyridine elaboration through organometallic intermediates: regiochemical control and completeness. *Chem. Soc. Rev.* **2007**, *36*, 1161–1172.
9. Ackermann, L.; Potukuchi, H. K.; Kapdi, A. R.; Schulzke, C., Kumada–Corriu Cross-Couplings with 2-Pyridyl Grignard Reagents. *Chem. Eur. J.* **2010**, *16*, 3300–3303.
10. Tobisu, M.; Hyodo, I.; Chatani, N., Nickel-Catalyzed Reaction of Arylzinc Reagents with N-Aromatic Heterocycles: A Straightforward Approach to C–H Bond Arylation of Electron-Deficient Heteroaromatic Compounds. *J. Am. Chem. Soc.* **2009**, *131*, 12070–12071.
11. Guo, P.; Joo, J. M.; Rakshit, S.; Sames, D., C–H arylation of pyridines: high

- regioselectivity as a consequence of the electronic character of C-H bonds and heteroarene ring. *J. Am. Chem. Soc.* **2011**, *133*, 16338–16341.
12. Ye, M.; Gao, G. L.; Edmunds, A. J.; Worthington, P. A.; Morris, J. A.; Yu, J. Q., Ligand-promoted C3-selective arylation of pyridines with Pd catalysts: gram-scale synthesis of (+/-)-preclamol. *J. Am. Chem. Soc.* **2011**, *133*, 19090–19093.
13. Murakami, K.; Yamada, S.; Kaneda, T.; Itami, K., C-H Functionalization of Azines. *Chem. Rev.* **2017**, *117*, 9302–9332.
14. Campeau, L.-C.; Rousseaux, S.; Fagnou, K., A Solution to the 2-Pyridyl Organometallic Cross-Coupling Problem: Regioselective Catalytic Direct Arylation of Pyridine N -Oxides. *J. Am. Chem. Soc.* **2005**, *127*, 18020–18021.
15. Wang, Z.; Li, K.; Zhao, D.; Lan, J.; You, J., Palladium-catalyzed oxidative C-H/C-H cross-coupling of indoles and pyrroles with heteroarenes. *Angew. Chem. Int. Ed.* **2011**, *50*, 5365 –5369.
16. Ackermann, L.; Fenner, S., Direct arylations of electron-deficient (hetero)arenes with aryl or alkenyl tosylates and mesylates. *Chem. Commun.* **2011**, *47*, 430–432.
17. Tan, Y.; Barrios-Landeros, F.; Hartwig, J. F., Mechanistic studies on direct arylation of pyridine N-oxide: evidence for cooperative catalysis between two distinct palladium centers. *J. Am. Chem. Soc.* **2012**, *134*, 3683–3686.
18. Mousseau, J. J.; Bull, J. A.; Charette, A. B., Copper-catalyzed direct alkenylation of N-iminopyridinium ylides. *Angew. Chem., Int. Ed.* **2010**, *49*, 1133 –1136.
19. Larivee, A.; Mousseau, J. J.; Charette, A. B., Palladium-Catalyzed Direct C-H Arylation of N -Iminopyridinium Ylides: Application to the Synthesis of (+)-Anabasine.

J. Am. Chem. Soc. **2008**, *130*, 52–54.

20. Ding, S.; Yan, Y.; Jiao, N., Copper-catalyzed direct oxidative annulation of N-iminopyridinium ylides with terminal alkynes using O₂ as oxidant. *Chem. Commun.* **2013**, *49*, 4250–4252.

21. Chau, S. T.; Lutz, J. P.; Wu, K.; Doyle, A. G., Nickel-catalyzed enantioselective arylation of pyridinium ions: harnessing an iminium ion activation mode. *Angew. Chem. Int. Ed.* **2013**, *52*, 9153 – 9156.

22. Berman, A. M.; Bergman, R. G.; Ellman, J. A., Rh(I)-catalyzed direct arylation of azines. *J. Org. Chem.* **2010**, *75*, 7863-8.

23. Schipper, D. J.; El-Salfiti, M.; Whipp, C. J.; Fagnou, K., Direct arylation of azine N-oxides with aryl triflates. *Tetrahedron.* **2009**, *65*, 4977–4983.

24. Preshlock, S. M.; Plattner, D. L.; Maligres, P. E.; Krska, S. W.; Maleczka, R. E., Jr.; Smith, M. R. I., A traceless directing group for C-H borylation. *Angew. Chem. Int. Ed.* **2013**, *52*, 13153 –13157.

25. Huang, X.; Huang, J.; Du, C.; Zhang, X.; Song, F.; You, J., N-oxide as a traceless oxidizing directing group: mild rhodium(III)-catalyzed C-H olefination for the synthesis of ortho-alkenylated tertiary anilines. *Angew. Chem. Int. Ed.* **2013**, *52*, 12970 –12974.

26. Luo, J.; Preciado, S.; Larrosa, I., Overriding ortho-para selectivity via a traceless directing group relay strategy: the meta-selective arylation of phenols. *J. Am. Chem. Soc.* **2014**, *136*, 4109–4112.

27. Zhang, F.; Spring, D. R., Arene C-H functionalisation using a removable/modifiable or a traceless directing group strategy. *Chem. Soc. Rev.* **2014**,

43, 6906–6919.

28. Zhang, F.-L.; Hong, K.; Li, T.-J.; Park, H.; Yu, J.-Q., Functionalization of C(sp³)–H bonds using a transient directing group. *Science*. **2016**, *351*, 252–256.

29. Besset, T.; Zhao, Q.; Poisson, T.; Pannecoucke, X., The Transient Directing Group Strategy: A New Trend in Transition-Metal-Catalyzed C–H Bond Functionalization. *Synthesis* **2017**, *49*, 4808–4826.

30. Gandeepan, P.; Ackermann, L., Transient Directing Groups for Transformative C–H Activation by Synergistic Metal Catalysis. *Chem* **2018**, *4*, 199–222.

31. Zeng, Y.; Zhang, C.; Yin, C.; Sun, M.; Fu, H.; Zheng, X.; Yuan, M.; Li, R.; Chen, H., Direct C–H Functionalization of Pyridine via a Transient Activator Strategy: Synthesis of 2,6-Diarylpyridines. *Org. Lett.* **2017**, *19*, 1970–1973.

32. Yamaguchi, A. D.; Chepiga, K. M.; Yamaguchi, J.; Itami, K.; Davies, H. M., Concise syntheses of dictyodendrins A and F by a sequential C–H functionalization strategy. *J. Am. Chem. Soc.* **2015**, *137*, 644–647.

33. Hwang, H.; Kim, J.; Jeong, J.; Chang, S., Regioselective introduction of heteroatoms at the C-8 position of quinoline N-oxides: remote C–H activation using N-oxide as a stepping stone. *J. Am. Chem. Soc.* **2014**, *136*, 10770–10776.

34. Ping, L.; Chung, D. S.; Bouffard, J.; Lee, S. G., Transition metal-catalyzed site- and regio-divergent C–H bond functionalization. *Chem. Soc. Rev.* **2017**, *46*, 4299–4328.

35. Ye, F.; Qu, S.; Zhou, L.; Peng, C.; Wang, C.; Cheng, J.; Hossain, M. L.; Liu, Y.; Zhang, Y.; Wang, Z. X.; Wang, J., Palladium-catalyzed C–H functionalization of acyldiazomethane and tandem cross-coupling reactions. *J. Am. Chem. Soc.* **2015**, *137*,

4435–4444.

36. Cheng, G. J.; Zhang, X.; Chung, L. W.; Xu, L.; Wu, Y. D., Computational organic chemistry: bridging theory and experiment in establishing the mechanisms of chemical reactions. *J. Am. Chem. Soc.* **2015**, *137*, 1706–1725.

37. Liu, W. B.; Schuman, D. P.; Yang, Y. F.; Toutov, A. A.; Liang, Y.; Klare, H. F. T.; Nesnas, N.; Oestreich, M.; Blackmond, D. G.; Virgil, S. C.; Banerjee, S.; Zare, R. N.; Grubbs, R. H.; Houk, K. N.; Stoltz, B. M., Potassium tert-Butoxide-Catalyzed Dehydrogenative C-H Silylation of Heteroaromatics: A Combined Experimental and Computational Mechanistic Study. *J. Am. Chem. Soc.* **2017**, *139*, 6867–6879.

38. Deng, C.; Lam, W. H.; Lin, Z., Computational Studies on Rhodium(III) Catalyzed C–H Functionalization versus Deoxygenation of Quinoline N-Oxides with Diazo Compounds. *Organometallics*. **2017**, *36*, 650–656.

39. Davies, D. L.; Macgregor, S. A.; McMullin, C. L., Computational Studies of Carboxylate-Assisted C-H Activation and Functionalization at Group 8-10 Transition Metal Centers. *Chem. Rev.* **2017**, *117*, 8649–8709.

40. Yang, Y. F.; Chung, L. W.; Zhang, X.; Houk, K. N.; Wu, Y. D., Ligand-controlled reactivity, selectivity, and mechanism of cationic ruthenium-catalyzed hydrosilylations of alkynes, ketones, and nitriles: a theoretical study. *J. Org. Chem.* **2014**, *79*, 8856–8864.

41. Zhang, X.; Chung, L. W.; Wu, Y. D., New Mechanistic Insights on the Selectivity of Transition-Metal-Catalyzed Organic Reactions: The Role of Computational Chemistry. *Acc. Chem. Res.* **2016**, *49*, 1302–1310.

42. Becke, A. D., Density - functional thermochemistry. III. The role of exact exchange. *The Journal of Chemical Physics. J. Chem. Phys.* **1993**, *98*, 5648–5652.
43. Lee, C.; Yang, W.; Parr, R. G., Development of the Colle-Salvetti correlation-energy formula into a functional of the electron density. *Phys. Rev. B.* **1988**, *37*, 785–789.
44. Hay, P. J.; Wadt, W. R., Ab initio effective core potentials for molecular calculations. Potentials for K to Au including the outermost core orbitals. *J. Chem. Phys.* **1985**, *82*, 299–310.
45. Fukui, K., A Formulation of the Reaction Coordinate. *J. Phys. Chem.* **1970**, *74*, 4161–4163.
46. Fukui, K., The Path of Chemical Reactions — The IRC Approach. *Acc. Chem. Res.* **1981**, *14*, 363–368.
47. Zhao, Y.; Truhlar, D. G., The M06 suite of density functionals for main group thermochemistry, thermochemical kinetics, noncovalent interactions, excited states, and transition elements: two new functionals and systematic testing of four M06-class functionals and 12 other functionals. *Theor. Chem. Account.* **2008**, *120*, 215–241.
48. Zhao, Y.; Truhlar, D. G., Density Functionals with Broad Applicability in Chemistry. *Acc. Chem. Res.* **2008**, *41*, 157–167.
49. Cheng, G.-J.; Song, L.-J.; Yang, Y.-F.; Zhang, X.; Wiest, O.; Wu, Y.-D., Computational Studies on the Mechanism of the Copper-Catalyzed sp³-C-H Cross-Dehydrogenative Coupling Reaction. *ChemPlusChem.* **2013**, *78*, 943–951.

50. Valero, R.; Costa, R.; Moreira, I. d. P. R.; Truhlar, D. G.; Illas, F., Performance of the M06 family of exchange-correlation functionals for predicting magnetic coupling in organic and inorganic molecules. *J. Chem. Phys.* **2008**, *128*, 114103,1–8.
51. Park, K.; Pak, Y.; Kim, Y., Large Tunneling Effect on the Hydrogen Transfer in Bis(μ -oxo)dicopper Enzyme: A Theoretical Study. *J. Am. Chem. Soc.* **2012**, *134*, 3524–3531.
52. Golub, I. E.; Filippov, O. A.; Gutsul, E. I.; Belkova, N. V.; Epstein, L. M.; Rossin, A.; Peruzzini, M.; Shubina, E. S., Dimerization Mechanism of Bis(triphenylphosphine)copper(I) Tetrahydroborate: Proton Transfer via a Dihydrogen Bond. *Inorg. Chem.* **2012**, *51*, 6486–6497.
53. Marenich, A. V.; Cramer, C. J.; Truhlar, D. G., Universal Solvation Model Based on Solute Electron Density and on a Continuum Model of the Solvent Defined by the Bulk Dielectric Constant and Atomic Surface Tensions. *J. Phys. Chem. B.* **2009**, *113*, 6378–6396.
54. Frisch, M. J. T., G. W.; Schlegel, H. B.; Scuseria, G. E.; Robb, M. A.; Cheeseman, J. R.; Scalmani, G.; Barone, V.; Mennucci, B.; Petersson, G. A.; Nakatsuji, H.; Caricato, M.; Li, X.; Hratchian, H. P.; Izmaylov, A. F.; Bloino, J.; Zheng, G.; Sonnenberg, J. L.; Hada, M.; Ehara, M.; Toyota, K.; Fukuda, R.; Hasegawa, J.; Ishida, M.; Nakajima, T.; Honda, Y.; Kitao, O.; Nakai, H.; Vreven, T.; Montgomery, J. A., Jr.; Peralta, J. E.; Ogliaro, F.; Bearpark, M.; Heyd, J. J.; Brothers, E.; Kudin, K. N.; Staroverov, V. N.; Kobayashi, R.; Normand, J.; Raghavachari, K.; Rendell, A.; Burant, J. C.; Iyengar, S. S.; Tomasi, J.; Cossi, M.; Rega, N.; Millam, J. M.; Klene, M.; Knox, J. E.; Cross, J. B.; Bakken, V.; Adamo, C.;

- Jaramillo, J.; Gomperts, R.; Stratmann, R. E.; Yazyev, O.; Austin, A. J.; Cammi, R.; Pomelli, C.; Ochterski, J. W.; Martin, R. L.; Morokuma, K.; Zakrzewski, V. G.; Voth, G. A.; Salvador, P.; Dannenberg, J. J.; Dapprich, S.; Daniels, A. D.; Farkas, Ö.; Foresman, J. B.; Ortiz, J. V.; Cioslowski, J.; Fox, D. J., *Gaussian 09, revision D.01; Gaussian, Inc.: Wallingford, CT, 2010*.
55. Yuan, R.; Lin, Z., Mechanism for the Carboxylative Coupling Reaction of a Terminal Alkyne, CO₂, and an Allylic Chloride Catalyzed by the Cu(I) Complex: A DFT Study. *ACS Catal.* **2014**, *4*, 4466–4473.
56. Ackermann, L., Carboxylate-Assisted Transition-Metal-Catalyzed C-H Bond Functionalizations: Mechanism and Scope. *Chem. Rev.* **2011**, *111*, 1315–1345.
57. Lapointe, D.; Fagnou, K., Overview of the Mechanistic Work on the Concerted Metallation–Deprotonation Pathway. *Chem. Lett.* **2010**, *39*, 1118–1126.
58. Berg, U.; Gallo, R.; Metzger, J., Demethylations of Quaternary Pyridinium Salts by a Soft Nucleophile, Triphenylphosphine. Electronic and Steric Accelerations. *J. Org. Chem.* **1976**, *41*, 2621–2624.
59. Aumann, D.; Deady, L. W., Simple Method for Demethylation of Quaternised Nitrogen Heterocyclic Compounds. *J. C. S. Chem. Comm.* **1973**, 32–33.
60. Kutney, J. P.; Greenhouse, R., The Protection and Deprotection of the Pyridine Nitrogen. *Synt. Comm.* **1975**, *5*, 119–124.